International Journal of Industrial Electronics, Control and Optimization © 2021 IECO
Vol. 4, No. 1, pp. 77-86, Jan (2021)

Design and Analysis of a New Topology of Rotor Magnets in Brushless DC Motors to Reduce Cogging Torque

Seyed Reza Mousavi-Aghdam[1,†], Amin Kholousi[2]

[1,2] Department of Electrical Engineering, University of Mohaghegh Ardabili, Ardabil, Iran

ABSTRACT

This paper presents a novel topology of permanent magnet brushless DC motors. Brushless DC motors usually experience torque ripple mainly caused by cogging torque. In the proposed motor, the whole structure of the rotor's permanent magnets has been changed so that the cogging torque is considerably mitigated. The philosophy behind this modification depends on the way of flux-path production in the rotor structure and it should be similar to the way of motor phases. An initial electromagnetic analysis is, first, carried out using the finite element method. A sensitivity analysis is, next, included to obtain the most important design parameters for the proposed structure. The different performance parameters of the motor are calculated and compared between the proposed structures and the conventional BLDC structures. The results reveal that the proposed motor has a considerably lower torque ripple retaining an average value of the produced torque. The proposed structure is also compared with an asymmetrical V-type structure and the results further show the effectiveness of the proposed structure.

Article Info

Keywords:
BLDC motor, Cogging torque, Finite element analysis, Magnetic topology

Article History:
Received 2020-06-06
Accepted 2020-08-15

I. INTRODUCTION

Nowadays brushless DC (permanent magnet) PM motors have been the main focus of many researchers because of their considerable advantages. In this type of AC motors, some PMs are used instead of field winding in the rotor structure and the phase windings are located on the stator. Generally, PM motor types including brushless DC motors, synchronous motors, and stepper motors are widely used in industrial/home applications and electric vehicles because of their high performance, low maintenance costs, low vibrations and acoustic noises. There are different types of magnet arrangements including inner and outer PMs that are located on the rotor side of the brushless motors. The internal PM rotor types have a proper mechanical structure in which the PMs are fixed in their positions when subjected to a centrifugal force at high speeds. Additionally, these types of brushless DC motors exhibit high torque density and high efficiency [1-3].

Because of the rotor magnetic configuration, brushless DC motors have inherently high cogging torque [4]. The cogging torque is produced by the interaction between the stator teeth and the rotor PM poles. Moreover, the cogging torque is an imposed undesirable torque that is usually called the torque without current and is a function of the rotor position. The periodicity of cogging torque depends on the number of the rotor poles and stator teeth. The main disadvantage of the cogging torque is the ripple exerted on the total torque. This causes not only vibration and noise but it may also influence the drive performance [5-6]. For some applications, the torque should be free of large ripples. These are the reasons why it has been important for the brushless DC motor designers to reduce cogging torque and then electromagnetic torque ripples are also undesired for the motor types that have no cogging torque [7]. Cogging torque may limit the use of different modern control techniques as well. Reference [8] explains a

[†]**Corresponding Author**: r.mousaviaghdam@uma.ac.ir
Tel: +98-4531505736, Fax: +98-4533512904, University of mohaghegh ardabili
Faculty of Engineering, University of Mohaghegh Ardabili, Ardabil, Iran

new method to overcome harmonic problems caused by cogging torque when field oriented control is used. However, these techniques can partly eliminate problems since cogging torque is inherently produced in BLDC motors.

There are many different methods in the literature aiming at reducing cogging torque. In some cases, a skewed structure is used in the PM designs [4]-[9], and in some others, an asymmetric PM design is the main contribution to reduce cogging torque [10-11]. Considering different rotor designs, one may conclude that there are two major categories in which the topology has been changed to reduce cogging torque. In the first category, only PM arrangements are changed [12-15] while in the second category, the shape of the PMs is modified [16-19]. The geometric optimization of the PMs is another issue that researchers are focused on. The optimization of the rotor pole width [20-25], and stator pole width [26-27], stator pole arc length [28] as well as the optimization of the rotor pole arc or stator tooth coefficients [29] are the main optimization challenges mitigating cogging torque. Many studies have been carried out on the rotor side, and this exhibits the importance of the rotor design in reducing of the cogging torque. Precise design of pole and tooth ratio [10], asymmetric design of rotor external diameter and the use of the modified pole shoe in the stator [30], reverse lamination [31], the creation of core gaps with different shapes, and an increase in the air gap length are the other recent attempts to reduce the cogging torque. In axial flux BLDC motors, the cogging torque may be differently reduced using some other techniques because different topology of the motor. There may be different layers in axial structure of BLDC motors to improve the cogging torque [32]. However, these techniques increase the 3D complexity of the BLDC motor design. Most of the mentioned methods help reduce peak-cogging torque. However, in most cases, this reduction of the cogging torque may not proportionally result in decreasing electromagnetic torque ripple.

This paper proposes a new rotor topology with a modified PM arrangement to considerably reduce cogging torque. In most cases, the reduction of the cogging torque may inappropriately influence some other characteristics, like average torque. This paper explains how the new design has no undesirable effect on the other motor parameters. The analysis is carried out using a finite element method (FEA) simulation, and the results are compared with that of a conventional brushless DC motor considering similar parameters. The comparison is additionally continued for a new structure like asymmetrical V-type configuration since this structure has already shown low cogging torque. The analysis results show that the proposed topology of brushless DC motors has considerably low cogging torque and, as a result, a low torque ripple while retaining the other main characteristics.

II. Cogging Torque in Brushless DC Motors

The torque produced in the PM motors is the result of the interaction between PM magnetic flux and the flux created by the windings. The total magnetic flux of a motor can be represented by the winding and PM fluxes, i.e. φ_w, φ_{PM}, respectively, as follows [33]:

$$\varphi_t = \varphi_w + \varphi_{PM} = \frac{N_w i_w}{\Re_w + \Re_{ag} + \Re_{PM}} + \frac{\varphi_r \Re_{PM}}{\Re_w + \Re_{ag} + \Re_{PM}} = \frac{N_w i_w}{\Re_t} + \frac{\varphi_r \Re_{PM}}{\Re_t} \quad (1)$$

where N_w and i_w are the winding turn number and current, respectively. $\Re_w$, $\Re_{ag}$, and $\Re_{PM}$ represent the reluctance of the winding core, air gap, and PMs, respectively. Also, φ_r is the internal flux of the permanent magnets linking the winding. It must be mentioned that the Eq. (1) is provided for a specified position and the winding reluctance, for example, is dependent on the position. In other words, Eq. (1) is based on the fluxes summation that dynamically changes. The winding inductance can be written as follows:

$$L_s = \frac{N_w^2}{\Re_w + \Re_{ag} + \Re_{PM}} = \frac{N_w^2}{\Re_t} \quad (2)$$

Hence, energy can be represented as follows:

$$W(i_w, \theta) = W_L + W_{PM} + W_w = \tfrac{1}{2} L_s i_w^2 + \tfrac{1}{2} \Re_t \varphi_{ag}^2 + N_w i_w \varphi_{PM} \quad (3)$$

where φ_{ag} is the air gap flux. Considering the energy equation, one can represent the produced torque as follows:

$$T = \frac{\partial W_c}{\partial \theta}\Big|_{i_w = cons.} = \tfrac{1}{2} i_w^2 \frac{dL_s}{d\theta} - \tfrac{1}{2} \varphi_{ag}^2 \frac{d\Re_t}{d\theta} + N_w i_w \frac{d\varphi_{PM}}{d\theta} \quad (4)$$

The first and third terms in the torque equation will be zero if no current is considered in motor windings. The cogging torque can, thus, be calculated using the following equation that is the interaction between the PM flux and stator tooth reluctance:

$$T_{cog} = \tfrac{1}{2} \varphi_{ag}^2 \frac{d\Re_t}{d\theta} \quad (5)$$

The mentioned cogging torque is inherently dictated by the motor geometric topology. The detailed explanations are given in the Sequent III.

III. Description of the Proposed Topology

Fig. 1 shows the proposed structure for brushless DC motors. To get some topological insight into the new design, the conventional structure of a motor is also illustrated. As shown in Fig. 1(a), the proposed topology utilizes an internal PM structure with four magnetic poles. The other pole

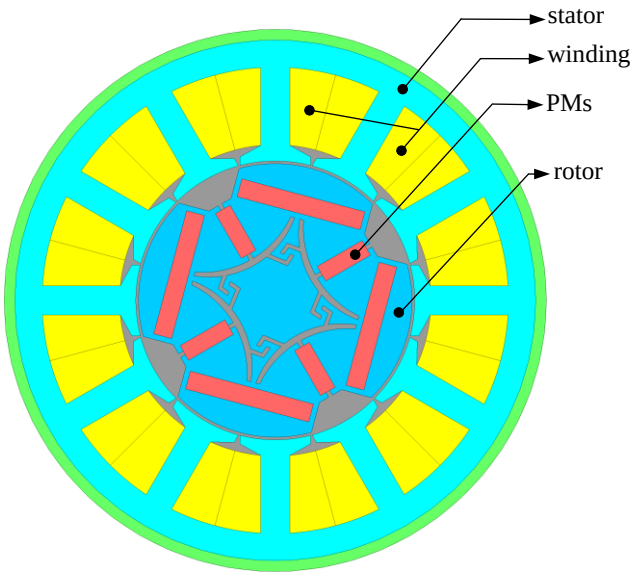

(a)

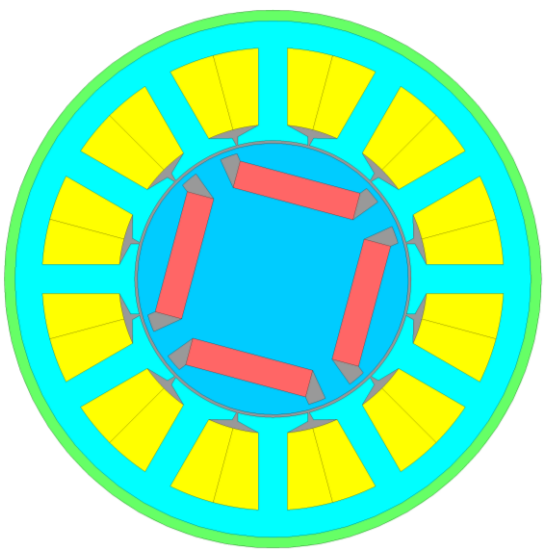

(b)

Fig. 1: (a) An illustration of proposed brushless DC motor along with its (b) conventional design.

combinations can, of course, be considered for the proposed topology. In the proposed topology, some different gaps are considered in the rotor core to conduct PM magnetic flux in a specified path. The PM dimension, shape, and orientation are also modified. The total size of the PM is not changed, and it is divided into some smaller PMs. These modifications are made to improve the flux path and maximize the performance of the PMs. To make the comparison more reasonable, it is assumed that the stator dimensions, winding structure, and total PM weight are the same in the proposed and conventional structures. Some other parameters are also assumed the same and summarized in Table I.

The proposed topology has different geometrical design parameters that may affect motor performance. To get an insight into the influences of these geometrical parameters, a sensitivity analysis is included in this section. Fig. 2 illustrates the proposed motor with its main geometric parameters that the topology is based on. Here, ml and mw are the length and width of the large magnets and sl and sw are the length and width of the small magnets, respectively. The point "O'" is the center of the arcs by which the guiding air gaps of the rotor magnetic flux are created. The large magnets have an angle shift of 90° from each other and the small magnets are located between them having an angle shift of 45° from the large magnets. On the internal sides of the rotor guiding air gaps, there are spiral air gaps by which the straight flowing of the magnetic flux is prevented. The final geometric parameter is the iron width, gw, which is considered to support the magnets and also to make the rotor body unified.

In the next step, the mentioned design parameters of the proposed BLDC motor are assessed using the sensitivity analysis. In this analysis, the dimensions of the magnets are modified in ten steps so that their total volume in each step remains constant. The parameter gw is also modified in five steps. The variation details are summarized in Table II.

Table I: Fixed parameters of the brushless DC motor

Parameter	Value
Nominal power, Voltage	350W, 80V
Rotor diameter	25.5mm
Stator external diameter	100mm
Stator internal diameter	26mm
Stack length	70mm
Air gap length	1mm
Stator tooth number	12
Pole number	4
Remanence of PMs	1.2T

The results of the sensitivity analysis for small magnet's dimensions of the proposed BLDC motor are illustrated in Fig. 3. As shown in Fig. 3 (a), when the width of the magnets is reduced and the length is, accordingly, increased, the phase produces more torque. However, for an appropriate length of the magnets, the torque change is negligible. The same can be seen for the cogging torque based on Fig. 3-(b). The results exhibit that the cogging torque is slightly low for wide magnets. In the next step, a similar analysis is carried out for the large magnets whose results are depicted in Fig. 4. As shown, the results for the large magnets are completely different in comparison to the small magnets. In this case, when the width of the magnets is reduced, the phase produces less torque. The same can be seen for the cogging torque in which higher values belong to the wider magnet. Comparing two sensitivity analyses, the results exhibit that the large magnet's dimensions have the most important effect on torque production. As a result, for a fixed volume of the large

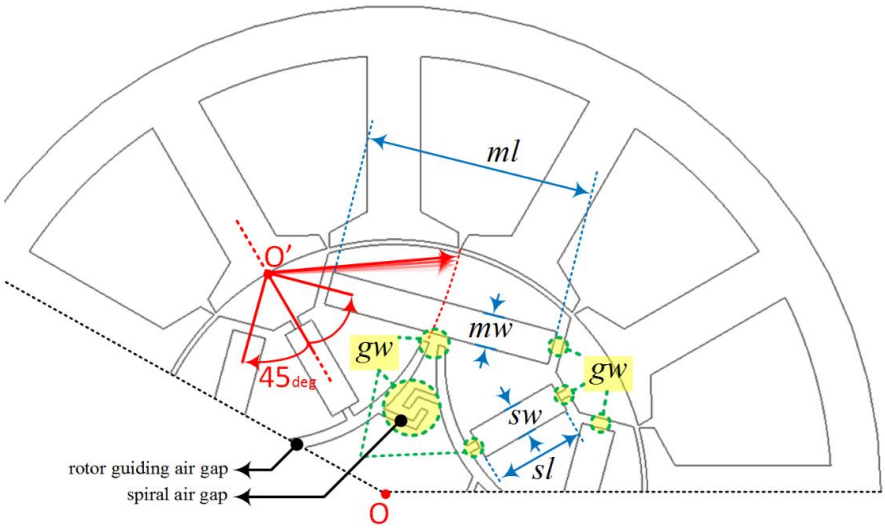

Fig. 2: Geometrical view of the proposed BLDC motor with main design parameters.

Table II: divisions of the main design parameters

Par.*/step	T1	T2	T3	T4	T5	T6	T7	T8	T9	T10	Vol.
sl	9.55	9.5	9.42	9.35	9.28	9.22	9.14	9.07	8.95	8.83	~30.3
sw	3.17	3.19	3.22	3.24	3.26	3.29	3.31	3.34	3.38	3.43	
ml	23.57	23.44	23.22	23.14	22.97	22.84	22.7	22.58	22.45	22.33	~81.7
mw	3.47	3.49	3.52	3.54	3.56	3.58	3.6	3.61	3.63	3.66	
gw	1.02	1.04	1.06	1.08	1.1	-	-	-	-	-	-

*All parameters are presented in mm

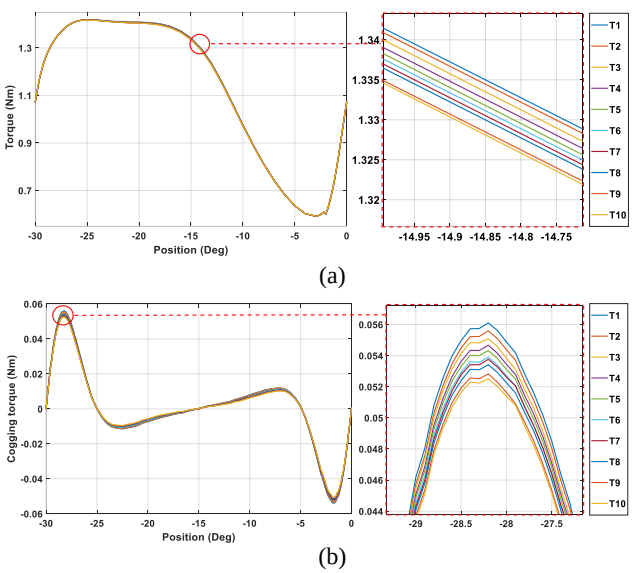

Fig. 3: (a) The produced torque and (b) cogging torque in terms of small magnet's dimensions.

magnets, widening of the magnets will lead to high torque. However, this results in high cogging torque as well. The geometric parameter, gw, is also considered in this analysis and the results are illustrated in Fig. 5 accordingly. The results show that widening the mentioned iron path will lead to low torque. On the other hand, there is always an optimum value for which the cogging torque is the lowest. Any increase/decrease from this optimum value will increase the cogging torque. The optimum value for this parameter in the proposed BLDC motor is about 1.05.

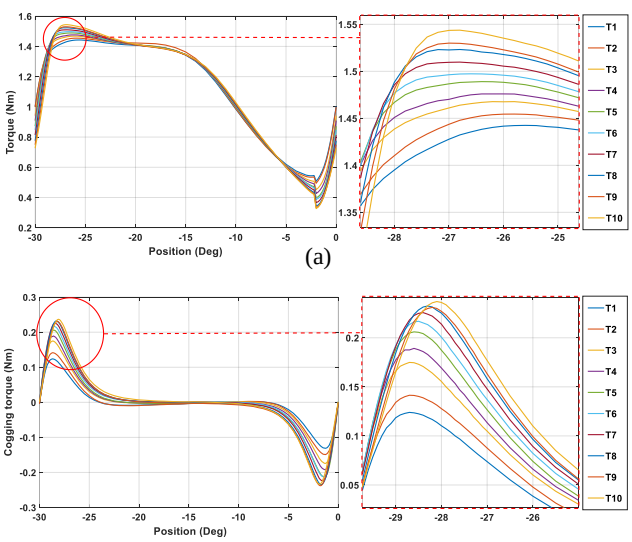

Fig. 4: (a) The produced torque and (b) cogging torque in terms of large magnet's dimensions.

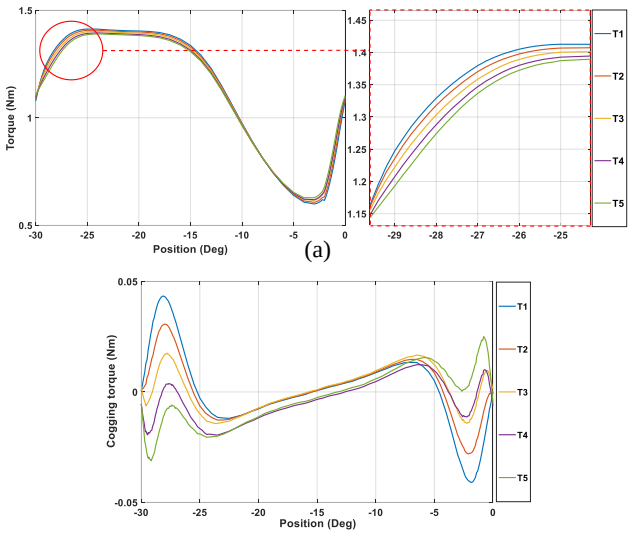

Fig. 5: (a) The produced torque and (b) cogging torque in terms of iron width *gw*.

IV. Performance Analysis and Comparisons

A. Analysis and Comparison with the Conventional Design

This section provides the results of an analysis of performance parameters for the proposed BLDC design in comparison to the conventional one. Fig. 6 shows the flux lines of the rotor permanent magnets flowing through the rotor and stator. The philosophy behind the proposed magnet topology is so that it produces the magnetic flux as similar as possible to the corresponding phase flux when no magnets are considered in the rotor. Fig. 6 shows the state of the flux path in the proposed structure while comparing it with the conventional flux path.

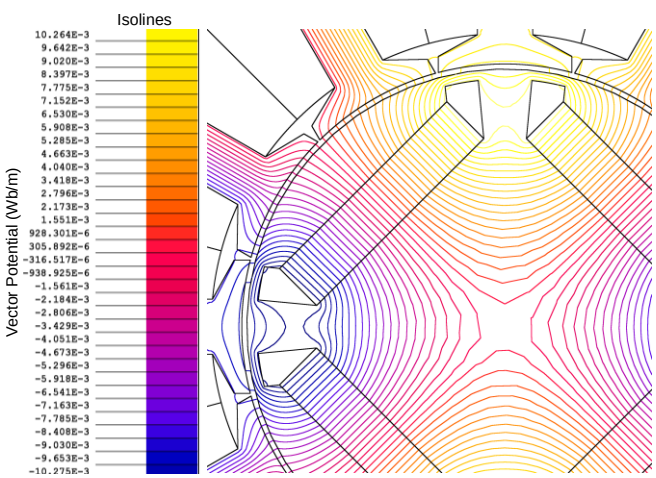

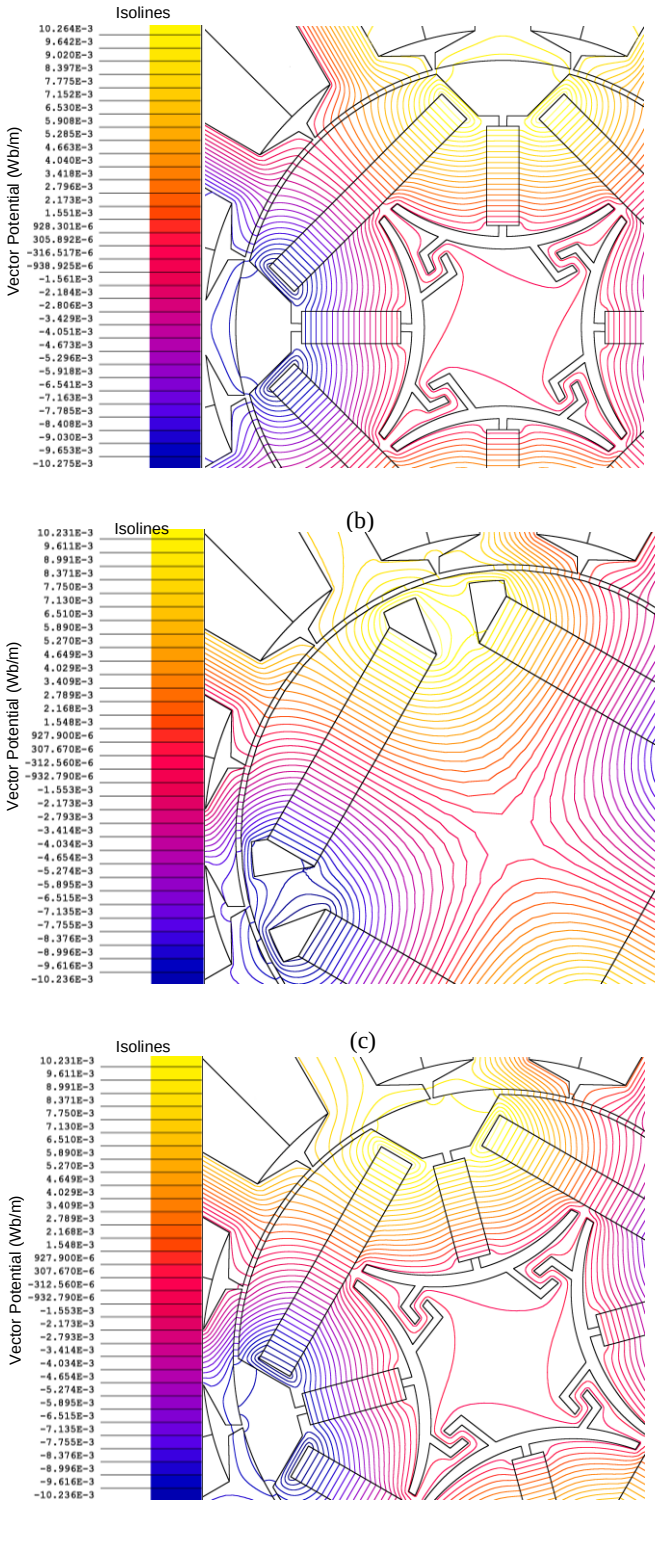

Fig. 6: The magnetic flux isolines of vector potentials for the proposed and conventional BLDC motors when PMs are aligned with two stator teeth (a), (b), and one stator tooth (c), (d).

Fig. 7 shows the air gap flux density. It is also shown that the maximum air gap flux density remains constant and this

possibility may prevent unwanted saturation of the stator teeth. Any changes in the mentioned flux density will affect the motor back-emf. How the flux has been changing determines the back-emf waveform. Fig. 8 shows the produced back-emf for the proposed and initial structure for a typical rotor speed. The back-emf waveform may influence the motor commutation and hence the motor total torque ripple. To precisely understand the difference in torque production capability of the proposed and conventional structure, the cogging and total torque of both motors are analyzed in the subsequent subsection.

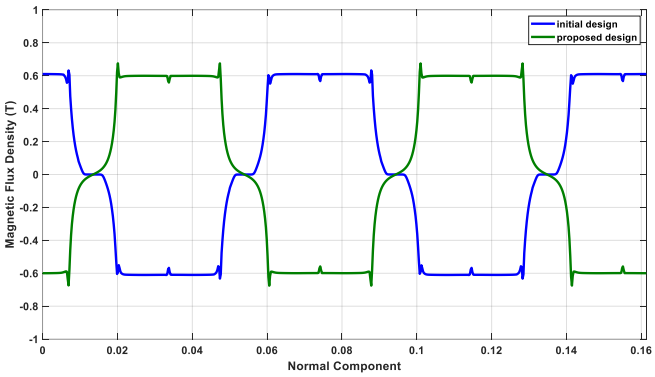

Fig. 7: The distribution of the air gap magnetic flux density in the proposed and conventional BLDC motors.

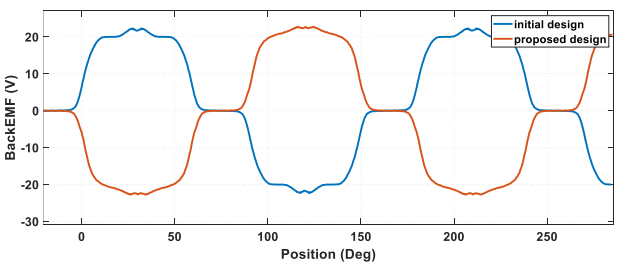

Fig. 8: A comparison of the produced back-emf for the proposed and initial structures.

The main contribution of the proposed BLDC motor is the reduction of cogging torque and hence electromagnetic torque. Fig. 9 compares the produced cogging torques of the proposed and conventional BLDC motors. As can be seen, the cogging torque for the proposed motor is considerably low and it has a small peak-to-peak value of 0.09Nm. This value for the conventional motor is about 0.29Nm and hence there has been a 70% reduction of in the cogging torque for the proposed BLDC motor. In this subsection, to assess the effectiveness of the proposed structure, a Fast Fourier Transform (FFT) analysis is also carried out to extract the cogging torque harmonics in both structures. The harmonic components of the cogging torque are illustrated in Fig. 10. The first to fourth harmonics play an important role in reducing cogging torque. Additionally, the proposed structure produces lower harmonics in comparison to the conventional one that may, in turn, result in a quiet operation and noise reduction in the proposed motor.

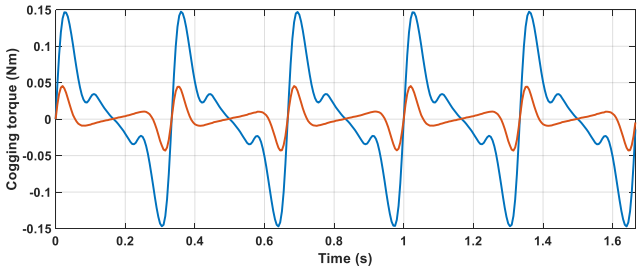

Fig. 9: A comparison of the cogging torque in the proposed and conventional BLDC motors.

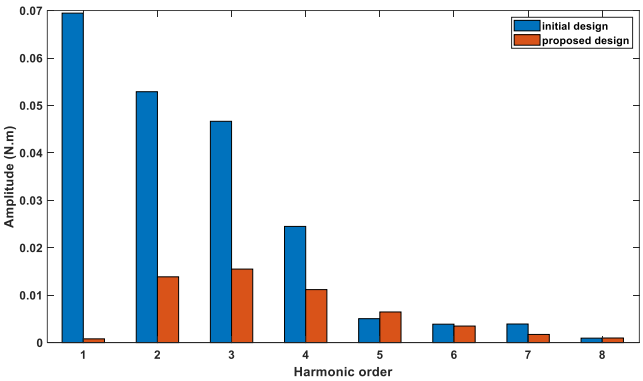

Fig. 10: The harmonic components of the cogging torque in the proposed and conventional motors.

There are different PM topologies that are used for BLDC motors to reduce the cogging torque, but most of them may cause unavoidably a reduction in the motor electromagnetic torque as well. Therefore, in any cogging torque improvement attempts, the electromagnetic torque retention must be considered. In this step, using a three-phase inverter, the proposed and conventional BLDC motors are energized, and the electromagnetic torque is obtained. The results are shown in Fig. 11 for a typical phase current of 4A. The average electromagnetic torque for the proposed and conventional motor is the same and is about 0.88Nm. As can be seen, the torque ripple is comparatively reduced in the proposed motor. The torque ripple for the proposed motor is 10.4% and for the conventional motor is 18%, which exhibits a 42% reduction for the proposed motor. The electromagnetic torque and ripple are verified for some other currents whose results are shown in Fig. 12. For lower values of the current, the average torque for both motors is the same (0.18Nm) but for high values of the current, electromagnetic torque of the proposed motor is slightly high (1.53Nm). Moreover, the torque ripple of the proposed motor for the lower value of the current is 9.1%, which is 60% lower than that of the conventional one. The torque ripple of the proposed motor for the higher values of the current is 13%, which is 27% lower than that of the conventional one. It should be mentioned that in the proposed

BLDC motor, the motor torque ripple is influenced by not only the cogging torque directly but also it is indirectly affected by the way of flux variation and back-emf waveforms. The latter may create torque ripple with the interaction between the back-emf and phase current. It should be mentioned that the iron loss pattern for the efficiency calculations is considered constant for both structures because of no considerable change in the magnetic field and iron volumes of the motors under discussion.

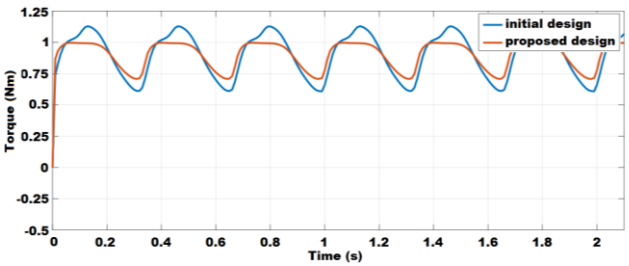

Fig. 11: An electromagnetic torque comparison of the proposed and conventional BLDC motors.

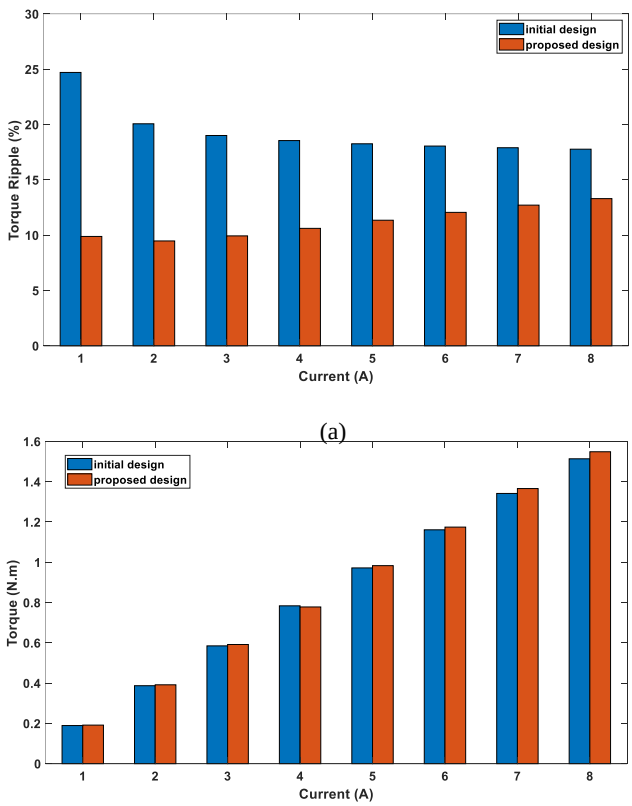

Fig. 12: (a) Electromagnetic torque and (b) torque ripple for the proposed and conventional BLDC motors in terms of motor currents.

B. Comparison with Asymmetrical V-type Design

In this section, a new comparative analysis is considered to assess the proposed design properly. Among the internal PM BLDC motors, V-type structures have some advantages. In [11], an asymmetrical V-type structure is introduced whose results confirm the reduction of the cogging and total torque in this structure. Therefore, the aforementioned structure is additionally considered in this paper. To make a reasonable comparison, the stator structure is the same as in the proposed motor, and an equal volume of PM is considered for the V-type structure. The value of other parameters in the mentioned structure is selected according to Table I. Fig. 13 shows the asymmetrical V-type design together with its magnetic flux lines.

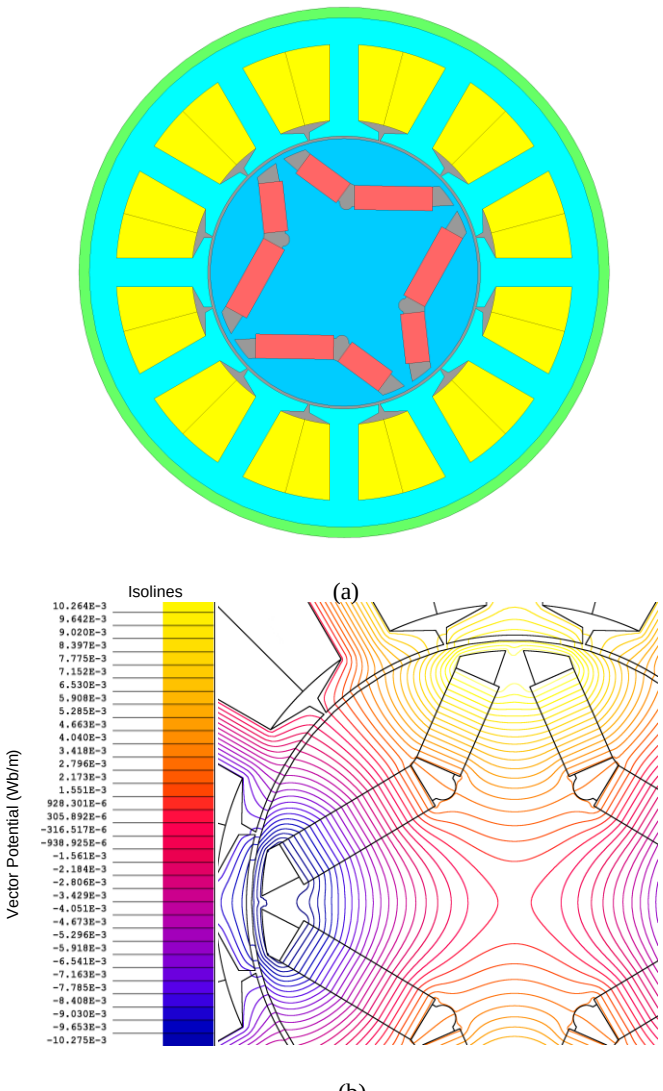

Fig. 13: (a) Asymmetrical V-type structure and (b) its magnetic flux lines.

In the next step, the back-emf is calculated for the asymmetrical V-type design and depicted in Fig. 14. In the back-emf flat area, the fluctuations are acceptable. As was already mentioned, torque ripple directly or indirectly depends on the cogging torque and this is comparatively shown in Fig. 15. The cogging torque for the proposed design is considerably low in comparison to the asymmetrical V-type structure.

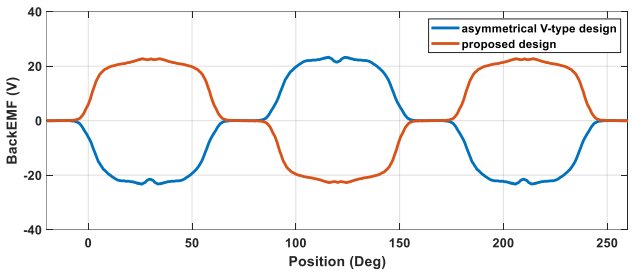

Fig. 14: A comparison of the produced back-emf for the proposed and asymmetrical V-type structures.

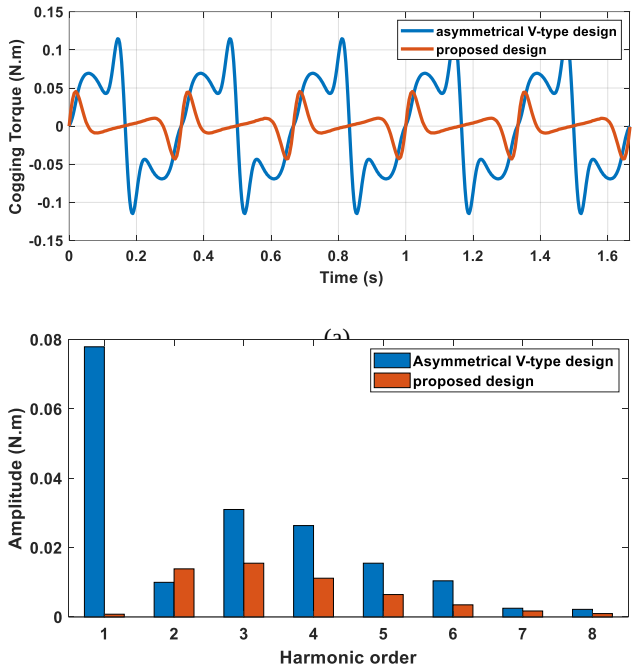

Fig. 15: A comparison of (a) the cogging torque and (b) its harmonic components in the proposed and asymmetrical V-type design.

In the next step, the motor torque is calculated for the asymmetrical V-type design and is depicted together with the torque of the proposed motor in Fig. 16. As shown, the proposed motor exhibits low torque ripple. Using different drive techniques, the torque ripple can be further reduced, but this paper focuses on the design of a geometrical topology. Finally, motor performance comparisons are summarized in Table III. The results confirm the effectiveness of the proposed BLDC motor structure. Considering the same configuration for the stator, the manufacturing cost of the proposed motor may be somehow different just because of the rotor structure. On the other hand, it is assumed that an equal volume of the PMs is used in the rotor configuration. Therefore, it seems that the cost difference will depend on the cutting method of the lamination and the number of PM segments as well. However, this difference may be neglected in a large scale production. The motor stack length in the proposed motor, as in internal PM BLDC motors, should be properly designed to ensure the mechanical robustness of the motor.

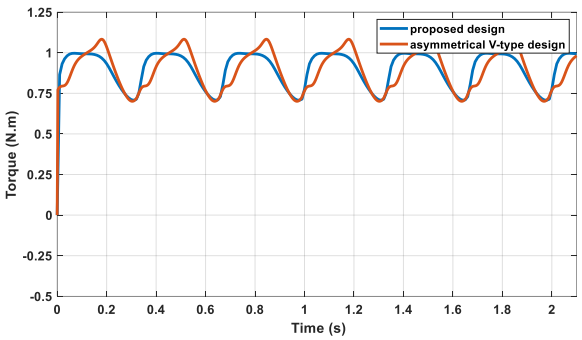

Fig. 16: An Electromagnetic torque comparison of the proposed and asymmetrical V-type designs.

Table III: Comparisons of the motor performance parameters

Parameter	Conventional BLDCM	Asymmetrical V-type BLDCM	Proposed BLDCM
Peak of cogging torque	0.29Nm	0.23Nm	0.09Nm
Average electromagnetic torque	0.882Nm	0.876Nm	0.88N.m
Torque ripple	18%	15%	10.4%
Efficiency	72.3%	74%	73.6%

V. Conclusion

This paper introduces a new permanent magnet brushless DC motor. Despite many advantages, torque ripple in BLDC motors is always a big concern for many researchers. The rotor structure together with the permanent magnet arrangement has a great impact on the cogging torque which often affects the torque ripple. This paper proposes and discusses a new BLDC structure in which the rotor is modified and permanent magnets are rearranged based on the magnetic flux path of the stator phases. The proposed structure has different geometric design parameters and in the first step, they are assessed by a sensitivity analysis. The main contribution of the proposed design is the considerable reduction of the torque ripple in comparison to conventional BLDC motors. More importantly, this torque ripple reduction has no undesirable effect on the main characteristics especially the mean torque. Since the proposed design introduces a new rotor PM configuration, it is additionally compared with another recent design of the rotor PM structure, i.e. asymmetrical V-type structure. In any case, the results exhibit low torque ripple for the proposed BLDC motor.

References

[1] Y. Chen, X. Zhu, L. Quan, Z. Xiang, Y. Du and X. Bu, "A V-Shaped PM Vernier Motor With Enhanced Flux-Modulated Effect and Low Torque Ripple," IEEE Trans. Magnetics, vol. 54, no. 11, pp. 1-4, Nov. 2018.

[2] Z. S. Du and T. A. Lipo, "Reducing Torque Ripple Using Axial Pole Shaping in Interior Permanent Magnet Machines," IEEE Trans. Industry Appl., vol. 56, no. 1, pp. 148-157, Jan.-Feb. 2020.

[3] Q. Chen, G. Xu, G. Liu, W. Zhao, L. Liu and Z. Lin, "Torque Ripple Reduction in Five-Phase IPM Motors by Lowering Interactional MMF," IEEE Trans. Ind. Electronics, vol. 65, no. 11, pp. 8520-8531, Nov. 2018.

[4] Bianchini, C., Immovilli, F., Lorenzani, E., Bellini, A., Davoli, M., "Review of design solutions for internal permanent-magnet machines cogging torque reduction," IEEE Trans. Magn., vol. 48, no. 10, pp. 2685 -2693, Oct. 2012.

[5] Hao, L., Lin, M., Xu, D., Li, N., Zhang, W., "Cogging torque reduction of axial-field flux-switching permanent magnet machine by rotor tooth notching," IEEE Trans. Magn., vol. 51, no. 11, pp.1-4, Nov. 2015.

[6] Zhao, W., Lipo, T.A., Kwon, B., "Torque pulsation minimization in spoke-type interior permanent magnet motors with skewing and sinusoidal permanent magnet configurations, IEEE Trans. Magn., vol. 51, no.11, pp.1-4, Nov. 2015.

[7] H. M. Cheshmeh-Beigi, A. Mohamadi, "Torque ripple minimization in SRM based on advanced torque sharing function modified by genetic algorithm combined with fuzzy PSO," International Journal of Industrial Electronics, Control and Optimization (IECO), vol. 1, no. 1, pp. 71-80, 2018.

[8] M. Sumega, P. Rafajdus, M. Stulrajter, "Current harmonics controller for reduction of acoustic noise, vibrations and torque ripple caused by cogging torque in PM motors under FOC operation," Energies, vol. 13, no. 10, pp. 1-23, May 2020.

[9] W. Fei, Z. Q. Zhu, "Comparison of Cogging Torque Reduction in Permanent Magnet Brushless Machines by Conventional and Herringbone Skewing Techniques," IEEE Trans. Energy Convers., vol. 28, no. 3, Sep. 2013.

[10] Gyu-Hong Kang, Young-Dae Son, Gyu-Tak Kim, Jin Hur, "A novel cogging torque reduction method for interior-type permanent-magnet motor," IEEE Trans. Ind. Appl., vol. 45, no. 1, Jan/Feb. 2009.

[11] Wu Ren, Qiang Xu, and Qiong Li, "Reduction of Cogging Torque and Torque Ripple in Interior PM Machines with Asymmetrical V-type Rotor Design," IEEE Trans. Magn., vol. 52, Jul. 2016.

[12] Keun-young Yoon, Byung-il Kwon, "Optimal Design of a New Interior Permanent Magnet Motor Using a Flared-Shape Arrangement of Ferrite Magnets," IEEE Trans. Magn., vol .52, Jul. 2016.

[13] D. Wang, X. Wang, M.-K Kim, and S.-Y. Jung, "Integrated optimization of two design techniques for cogging torque reduction combined with analytical method by a simple gradient descent method," IEEE Trans. Magn., vol. 48, no. 8, pp. 2265–2276, Aug. 2012.

[14] L. Dosiek and P. Pillay, "Cogging torque reduction in permanent-magnet machines," IEEE Trans. Ind. Appl., vol. 43, no. 6, pp. 1565–1571, Nov./Dec. 2007.

[15] T. Tudorache and I. Trifu, "Permanent-magnet synchronous machine cogging torque reduction using a hybrid model," IEEE Trans. Magn., vol. 48, no. 10, pp. 2627–2632, Oct. 2012.

[16] N. Chen, S. L. Ho, and W. N. Fu, "Optimization of permanent magnet surface shapes of electric motors for minimization of cogging torque using FEM," IEEE Trans. Magn., vol. 46, no. 6, pp. 2478–2481, Jun. 2010.

[17] S. M. Hwang, J.-B. Eom, Y.-H. Jung, D.-W. Lee, and B.-S. Kang, "Various design techniques to reduce cogging torque by controlling energy variation in permanent magnet motors," IEEE Trans. Magn., vol. 37, no. 4, pp. 2806–2809, Jul. 2001.

[18] M. R. Dubois, H. Polinder, and J. A. Ferreira, "Magnet shaping for minimal magnet volume in machines," IEEE Trans. Magn., vol. 38, no. 5, pp. 2985–2987, Sep. 2002.

[19] Hsing-Cheng Yu, Bo-Syun Yu, Jen-te Yu, and Cheng-Kai Lin, "A Dual Notched Design of Radial-Flux Permanent Magnet Motors with Low Cogging Torque and Rare Earth Material," IEEE Trans. Magn., vol. 50, no. 11, Nov. 2014.

[20] W. Fei, P. C. K. Luk, J. X. Shen, B. Xia, and Y.Wang, "Permanent-magnet flux-switching integrated starter generator with different rotor configurations for cogging torque and torque ripple mitigations," IEEE Trans. Ind. Appl., vol. 47, no. 3, pp. 1247–1256, May/Jun. 2011.

[21] Z. Q. Zhu and D. Howe, "Influence of design parameters on cogging torque in permanent magnet machines," IEEE Trans. Energy Convers., vol. 15, no. 4, pp. 407–412, Dec. 2000.

[22] W. Fei and P. C. K. Luk, "A new technique of cogging torque suppression in direct-drive permanent-magnet brushless machines," IEEE Trans. Ind. Appl., vol. 46, no. 4, pp. 1332–1340, Jul./Aug. 2009.

[23] N. Bianchi and S. Bolognani, "Design techniques for reducing the cogging torque in surface-mounted PM motors," IEEE Trans. Ind. Appl., vol. 38, no. 5, pp. 1259–1265, Sep./Oct. 2002.

[24] T. Li and G. Slemon, "Reduction of cogging torque in permanent magnet motors," IEEE Trans. Magn., vol. 24, no. 6, pp. 2901–2903, Nov. 1988.

[25] Y. Yang, X. Wang, R. Zhang, T. Ding, and R. Tang, "The optimization of pole-arc coefficient to reduce cogging torque in surface-mounted permanent magnet motors," IEEE Trans. Magn., vol. 42, no. 4, pp. 1135–1138, Apr. 2006.

[26] B. Ackermann, J. H. H. Janssen, R. Sotteck, and R. I. van Steen, "New technique for reducing cogging torque in a class of brushless DC motors," Proc. IEE—Electr. Power Appl., vol. 139, no. 4, pp. 315–320, Jul. 1992.

[27] X. Jiang, J. Xing, Y. Li, and Y. Lu, "Theoretical and simulation analysis of influences of stator tooth width on cogging torque of BLDC motors," IEEE Trans. Magn., vol. 45, no. 10, pp. 4601–4604, Oct. 2009.

[28] L. Petkovska, P. Lefley, G. V. Cvetkovski, "Design techniques for cogging torque reduction in a fractional-slot PMBLDC motor," COMPEL-The international journal for computation and mathematics in electrical and electronic engineering, vol. 39, no. 3, May 2020.

[29] Zhu,Z.Q., Ruangsinchaiwanich, S., Schofield, N., Howe, D., "Reduction of cogging torque in interior-magnet brushless machines," IEEE Trans. Magn., vol. 39, no. 5, pp. 3238-3240, Sept. 2003.

[30] Sun-Kwon Lee, Gyu-Hong Kang, Jin Hur, Byoung-Woo Kim, "Stator and rotor shape designs of interior permanent magnet type brushless DC motor for reducing torque fluctuation," IEEE Trans. Magn., vol.48, no.11, pp.4662,4665, Nov. 2012.

[31] Ki-Chan Kim, "A novel method for minimization of cogging torque and torque ripple for interior permanent magnet synchronous motor," IEEE Trans. Magn., vol. 50, no. 2, pp. 793-796, Feb. 2014.

[32] A. N. Patel, B. N. Suthar, "Double layer magnet design technique for cogging torque reduction of dual rotor single stator axial flux brushless DC motor," Iranian Journal of Electrical and Electronic Engineering (IJEEE), vol. 16, no. 1, pp. 58-65, Mar. 2020.
[33] D. C. Hanselman, Brushless Permanent Magnet Motor Design, 2nd ed. Cranston, RI, USA: The Writers' Collective, 2003.

Seyed Reza Mousavi-Aghdam received his B.Sc. degree with first-class honor from the Azarbaijan University of Shahid Madani in 2009, Tabriz, Iran, and M.Sc. and Ph.D. Degrees from the University of Tabriz, Iran, in 2011 and 2015 respectively all in Electrical Engineering. From September 2014 to March 2015, he has been a visiting research scholar at the Department of Industrial Engineering, University of Padova, Italy. Since 2016, he has joined the Department of Electrical Engineering, University of Mohaghegh Ardabili, Ardabil, Iran, as an assistant professor. His current research interests include design of electrical machines, electric drives, and analysis of special electrical machines.

Amin Kholousi was born in Ardabil, Iran. He received his B.Sc. degree in Electrical Engineering from the University of Mohaghegh Ardabili, Ardabil, Iran, in 2020. His current research interests include electric machines, modeling, and design of permanent-magnet machines.